First published August 16, 2016; doi:10.1152/ajpendo.00166.2016.

CALL FOR PAPERS | *CNS Control of Metabolism*

Central GIP signaling stimulates peripheral GIP release and promotes insulin and pancreatic polypeptide secretion in nonhuman primates

Paul B. Higgins,[1,2] Robert E. Shade,[2] Irám P. Rodríguez-Sánchez,[3] Magdalena Garcia-Forey,[2] M. Elizabeth Tejero,[4] V. Saroja Voruganti,[5] Shelley A. Cole,[1] Anthony G. Comuzzie,[1,2] and Franco Folli[2,6,7,8]

[1]*Department of Genetics, Texas Biomedical Research Institute, San Antonio, Texas;* [2]*Southwest National Primate Research Center, San Antonio, Texas;* [3]*Department of Genetics, School of Medicine, Autonomous University of Nuevo León (Universidad Autonoma de Nuevo León), Monterrey, Nuevo León, Mexico;* [4]*Laboratory of Nutrigenetics and Nutrigenomics, National Institute of Genomic Medicine (Instituto Nacional de Medicina Genómica), Mexico City, Mexico;* [5]*Department of Nutrition and UNC Nutrition Research Institute, University of North Carolina at Chapel Hill, Kannapolis, North Carolina;* [6]*Diabetes Division, Department of Medicine, University of Texas Health Sciences Center at San Antonio, San Antonio, Texas;* [7]*Department of Medicine, Obesity and Comorbidities Research Center, University of Campinas, Campinas, São Paulo, Brazil; and* [8]*Dipartimento di Scienze della Salute, Università degli Studi di Milano, Milan, Italy*

Submitted 27 April 2016; accepted in final form 10 August 2016

Higgins PB, Shade RE, Rodríguez-Sánchez IP, Garcia-Forey M, Tejero ME, Voruganti VS, Cole SA, Comuzzie AG, Folli F. Central GIP signaling stimulates peripheral GIP release and promotes insulin and pancreatic polypeptide secretion in nonhuman primates. *Am J Physiol Endocrinol Metab* 311: E661–E670, 2016. First published August 16, 2016; doi:10.1152/ajpendo.00166.2016.—Glucose-dependent insulinotropic polypeptide (GIP) has important actions on whole body metabolic function. GIP and its receptor are also present in the central nervous system and have been linked to neurotrophic actions. Metabolic effects of central nervous system GIP signaling have not been reported. We investigated whether centrally administered GIP could increase peripheral plasma GIP concentrations and influence the metabolic response to a mixed macronutrient meal in nonhuman primates. An infusion and sampling system was developed to enable continuous intracerebroventricular (ICV) infusions with serial venous sampling in conscious nonhuman primates. Male baboons (*Papio* sp.) that were healthy and had normal body weights (28.9 ± 2.1 kg) were studied ($n = 3$). Animals were randomized to receive continuous ICV infusions of GIP (20 pmol·kg^{-1}·h^{-1}) or vehicle before and over the course of a 300-min mixed meal test (15 kcal/kg, 1.5g glucose/kg) on two occasions. A significant increase in plasma GIP concentration was observed under ICV GIP infusion (66.5 ± 8.0 vs. 680.6 ± 412.8 pg/ml, $P = 0.04$) before administration of the mixed meal. Increases in postprandial, but not fasted, insulin ($P = 0.01$) and pancreatic polypeptide ($P = 0.04$) were also observed under ICV GIP. Effects of ICV GIP on fasted or postprandial glucagon, glucose, triglyceride, and free fatty acids were not observed. Our data demonstrate that central GIP signaling can promote increased plasma GIP concentrations independent of nutrient stimulation and increase insulin and pancreatic polypeptide responses to a mixed meal.

glucose-dependent insulinotropic polypeptide; brain; intracerebroventricular; nonhuman primate

GLUCOSE-DEPENDENT INSULINOTROPIC POLYPEPTIDE (GIP) is a 42-amino acid peptide released primarily from enteroendocrine K cells in response to nutrient stimulation. Although originally described for its role in gastric acid secretion (5), GIP is an important incretin peptide and an essential driver of normal postprandial insulin secretion (17). Beyond its insulinotropic and intestinal actions, GIP also has effects on adipose tissue, bone, the heart and vasculature, pancreatic α-cells, and, importantly, the central nervous system (8).

The GIP receptor (GIPR) is expressed in multiple regions of the mammalian brain (32, 45), and immunohistochemically detected GIP has also been shown in the rat brain (36). Brain GIP action is now linked to neurotrophic effects and augmented synaptic plasticity in rodents (20–22, 29, 31, 39, 44, 53). Whether central GIP signaling can generate effects outside of the central nervous system is unclear (2, 16, 38). In support of such an action for GIP, other metabolically active intestinal peptides (6, 41) are known to generate peripheral effects through actions in the brain and, thereby, modulate metabolic function through the gut-brain axis.

A series of recent studies in a canine model has provided evidence for a brain-gut signaling pathway capable of modulating GIP concentrations in the peripheral circulation. These studies showed that plasma GIP concentrations were increased by intracerebroventricular (ICV) administration of neuropeptide Y (48), bombesin (51), and neurotensin (50) and decreased by ICV insulin (49). Earlier studies also demonstrated nutrient-independent effects of bombesin-like peptides on GIP release in enteroendocrine cell lines, suggesting an independent neural influence on GIP secretion from K cells (35). Combined, these studies support a role for neuroregulation in peripheral GIP release and indicate the presence of an efferent signal from the brain to the gut that can modulate GIP release independent of nutrient stimulation.

We investigated whether centrally administered GIP could increase peripheral plasma GIP concentrations and influence the metabolic response to a mixed macronutrient meal in conscious healthy nonhuman primates. Here, we present evidence that central nervous system GIP signaling generates an efferent signal that stimulates GIP release into the peripheral circulation and influences postprandial islet peptide secretion.

Current address for reprint requests and other correspondence: P. B. Higgins, Sichuan PriMed Biotech Ltd., B4-501 Tianfu Life Science Technology Park, Chengdu, Sichuan, China (e-mail: paulb.higgins@gmail.com).

METHODS

Test subjects. Four healthy young adult male baboons (*Papio* sp.*)* were originally selected for study; $n = 3$ animals completed the study protocol. Before the initiation of study activities, all animals were housed in social groups in outdoor enclosures at the Southwest National Primate Research Center according to the National Institutes of Health *Guide for the Care and Use of Laboratory Animals*. All animals were then transferred to a vivarium and housed in species-appropriate metabolic cages and were maintained at constant room temperature and humidity in a 12:12-h light-dark cycle for the duration of the study activities. The indoor housing environment was enriched using food items, food puzzles, chewable toys, audio, and visual tools according to Association for Assessment and Accreditation of Laboratory Animal Care guidelines. A licensed veterinarian performed a standard health assessment including a physical examination and serum chemistry and hematology profiling in all animals before their inclusion in the study. All animals were healthy with no history of medical illness. Animals were fed a standard nonhuman primate diet [5LE0 solid feed, LabDiet, PMI, St. Louis, MO; this diet contains 3.26 kcal/g with 13.8% fat, 67.2% carbohydrate (3% sugar), and 19% protein as a percentage of total energy] between 0800 and 1800 daily and had continuous access to water. All study procedures were approved by the Institutional Animal Care and Use Committee of the Texas Biomedical Research Institute (San Antonio, TX).

Tether system adaptation period. After an initial period of acclimation to the indoor housing environment, $n = 12$ animals (initial selection pool) were evaluated for adaptation to single caging and to the presence of a tether jacket and tether coil for a period of 3 wk. This "sham tethering" approach has been described in detail elsewhere (14). In brief, each animal was fitted to a customized cotton tether jacket that was connected to a stainless steel coil that "tethered" the animal to the cage ceiling. During this period, animals were assessed daily for behavior and food intake and were sedated weekly for physical and biochemical health assessments and to enable adjustments to the tethering system to ensure optimal comfort and functionality. Four animals were selected based on technician- and investigator-determined habituation to the housing environment and tether system. These animals then underwent the following procedures in preparation for study: *1*) presurgical stereotaxic brain coordinate identification, *2*) implant of a lateral cerebral ventricular cannula, and *3*) femoral vein catheterization surgery and connection of ventricular and venous lines through the system. An overview of the study is shown in Fig. 1, *top*. The experiments undertaken involved modification of an extant vascular infusion and sampling system (3, 14) to enable ICV infusion in alert singly caged nonhuman primates (27) and are detailed below.

Presurgical stereotaxic brain coordinate identification. The selected animals were prepared for ICV cannulation surgery. Each baboon was sedated with ketamine (10 mg/kg im) and fitted to a stereotaxic frame (model 1504, dog and monkey stereotaxic frame, David Kopf Instruments, Tujunga, CA). The frame is designed to enable the baboon to lie in a prone position with the head raised above shoulder height. This initial fitting procedure was used to establish and record accurate coordination points for cannula implant in the left lateral cerebral ventricle of each animal. Specifically, the stereotaxic frame was adjusted so that the lower edge of the frame's eye rods was parallel (in the same plane) to the center of the ear bars, thus establishing a horizontal plane zero reference point for each animal that was consistent with the Baboon Brain Atlas (15). Following from this, the coordinates for the exact midpoint between the ends of the ear bars were identified to establish the anterior-posterior zero-point coordinate and the lateral left-to-right zero coordinate for the brain of each animal. Animals were returned to their home cages immediately after the coordinates were identified and recorded.

ICV cannula implant surgery. Seven days after stereotaxic coordinate identification procedures, each animal was sedated with ketamine (10 mg/kg im) and transported to a surgery room for ICV implant surgery. Details of the ICV cannula implant surgery in baboons in our laboratory have been previously published (3, 4, 43). Anesthesia was induced and maintained with isoflurane inhalation [1.0–1.5% (vol/vol)]. The stereotaxic frame was positioned according to the previously determined coordinates. Based on the identification of the region of the lateral cerebral ventricle during frame fitting, a midline incision along with blunt dissection was made to expose the cranium. A hole (5-mm diameter) was drilled through the cranium at 19 mm anterior to the ear bar and 1.0 mm left of the midline. The *z*-coordinate location of the dura was then established by lowering the tip of the cannula until it made contact with the dura. At this time, a pressure transducer (SensorMedics, Yorba Linda, CA) was connected to record hydrostatic pressure within the cannula. Sterile 0.9% NaCl solution was infused through the cannula at a rate of 5 ml/h as the cannula was slowly lowered in 1-mm increments through the cerebral tissue. Hydrostatic pressure within the cannula was recorded in real time using a strip chart recorder. The location of the lateral cerebral was determined at the *z*-coordinate where hydrostatic pressure inside the cannula decreased to zero. Lateral ventricular cannula placement was then confirmed by fluoroscopic imaging of the lateral ventricular space during delivery of a 1-ml bolus of iohexol (Omnipaque, GE Healthcare, Princeton, NJ) through the cannula. All cannulas were confirmed to be positioned in the lateral cerebral ventricle. The location of the lateral cerebral ventricle was between 20 and 25 mm inferior to the dura in all animals. The cannula was then fixed in place by placing dental acrylic in and around the cranial hole. The external

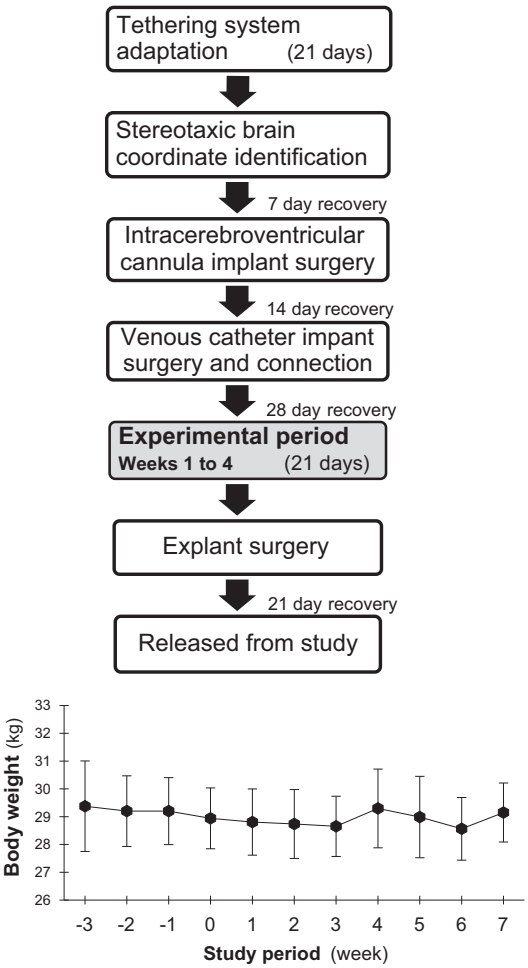

Fig. 1. Study design. *Top*: study procedure overview. *Bottom*: body weight stability. Data are means ± SE; $n = 3$.

portion of the cannula was slowly pushed downward at a right angle and positioned parallel to the surface of the skull. To anchor the dental acrylic, self-tapping stainless steel screws were placed in the cranium next to the cannula and additional dental acrylic was added to allow sufficient coverage of the screws and the cannula. Twenty-gauge polyvinyl tubing (Tygon S54HL microbore tubing, St. Gobain, Akron, OH) was attached to the external end of the cannula and routed subcutaneously to an exit site on the lower back of the animal. The ventricular cannula line was slowly loaded with artificial cerebrospinal fluid (aCSF) and connected to a miniosmotic pump containing aCSF (Alzet, Palo Alto, CA), which was then implanted subcutaneously to maintain the patency of the ventricular infusion line and cannula before connection to the infusion system, as previously described (3). The cranial incision was closed with a 3-0 polyglactin suture (Vicryl, Ethicon) so that the skin completely covered the cannula and acrylic block. The incision site for the pump was closed with a 3-0 suture (Vicryl, Ethicon). Animals were then returned to their home cages for recovery.

ICV cannula surgery perioperative medications. Thirty minutes before the surgical incision, each animal received a prophylactic dose of Cefazolin (350 mg iv). Tramadol was administered intraoperatively at a continuous infusion at a rate of 150 μg/kg iv. Animals were monitored continuously for 12 h in the immediate postoperative period. Postoperatively, animals were dosed further with Tramadol either with the injectable or oral form twice daily and received a single dose of Zofan (2 mg). Cefazolin (25 mg/kg) was administered intravenously twice per day for 5 days after surgery.

Femoral vein catheterization surgery. Fourteen days after the ICV cannula implant surgery was performed, a second surgery was performed to implant a catheter (5-Fr Hydrocoat, Access Technologies, Skokie, IL) in the femoral vein for sampling. Animals were sedated with ketamine HCl (10 mg/kg im), and gas anesthesia was induced and maintained using isoflurane [1.0–1.5% (vol/vol)]. A catheter was then implanted in the femoral vein via a skin incision over the femoral vessels in the femoral triangle of the inner thigh. This catheter was then routed subcutaneously to the midscapular region of the back to exit the skin at the location of the tether jacket backpack box and locked using a syringe containing sterile 0.9% NaCl. The osmotic pump was explanted and disconnected from the ICV line, and the ICV line was also routed subcutaneously through an additional exit site made ~10 cm superior to that of the venous line and locked using sterile 0.9% NaCl.

Venous catheter implants surgery perioperative medications. During surgery, animals were given a prophylactic analgesic (0.2 mg/kg Metacam) and prophylactic antibiotic (25 mg/kg Cephazolin). After surgery, Buprinex was administered (0.01 mg/kg qid) for 3 days and antibiotic treatment [Cephazolin (25 mg/kg bid)] was continued for 7 days.

Connection of ICV infusion and venous sampling lines. After surgery, animals were returned to their home cages. While the animals remained under sedation, the venous catheter was connected through the tethering system and kept patent using a continuous heparinized saline (5 U/ml) infusion from a volumetric infusion pump maintained at the top of the cage, as previously described (14). In parallel, the ICV infusion line was also routed through the tether coil to the infusion system at the top of the cage. The ICV line was kept patent using a continuous infusion of aCSF (10 μL/h) through a network syringe pump (New Era Pump Systems, Farmingdale, NY), as described below. The ICV line was connected through a pressure transducer positioned inside the tether jacket backpack box at this time, as has been previously described for arterial lines (3). The line dead space was also measured at this time. A 4-wk recovery period was provisioned after the femoral catheter implant surgery and before the initiation of the experimental period. All animals underwent detailed weekly physical, biochemical, and hematological health examinations under ketamine sedation throughout the postsurgery and experimental periods. The physical examination was conducted by a veterinarian and involved detailed inspection of the venous and ventricular line exit site. Animal behavior was observed remotely using a closed circuit network camera mounted on the wall opposite the animal's cage. No evidence for pain, distress, or malaise was observed during the ICV infusion experiments.

ICV infusion system. We modified the aforementioned established tethering system (14), which enables blood sampling and intravenous infusion in singly caged conscious baboons, to include an ICV line accessible from the cage exterior. As noted above, the cannula line was routed through an exit site in the lower back region and was connected through the stainless steel tether coil to the infusion apparatus at the top of the cage. A continuous infusion of aCSF at 10 μl/h was maintained through ICV infusion line using a Bluetooth-modified network syringe pump (New Era Pump Systems) that was attached to the tether mast at the top of the cage. ICV pumps were controlled remotely using computer software (Syringe Pump Pro, TBITC, Adelaide, SA, Australia) located in a room adjacent to the animal housing rooms. To confirm patency of the ICV cannula throughout the study, data from the ICV line pressure transducer were acquired and continuously recorded using a Ponemah Physiology Platform with P3 Plus Software for Windows (LDS Test Measurement and Gould Instrument Systems, Valley View, OH). Any blockage or disconnection in the ICV line was registered as an increase or drop in line pressure, respectively. All ICV infusions were delivered through a 0.20 μm syringe filter unit attached to the syringe.

Animal habituation. Extensive habituation of the animals to technician presence was conducted at regular intervals during the 4-wk recovery period. Animals were fully habituated to serial blood sampling and to the mixed meal administration on 2 occasions/wk. All experiments were performed by the same team of technicians and investigators who worked with the baboons on a daily basis throughout the entire prestudy and experimental period. One animal failed to adapt to the tether system and was removed from study before initiation of the experimental phase. The remaining animals ($n = 3$) adapted fully to the tether system, had normal food and water intakes, and were weight stable before initiation of the mixed meal metabolic experiments.

GIP peptide. Human GIP (1–42) peptide (Bachem, Torrence, CA) was used for ICV infusion. Peptide was added to aCSF vehicle with corrections for purity. We have found that the GIP (1–42) peptide coding region of the baboon GIP gene has 100% identity with the human ortholog. Baboon and human GIPR gene exon sequences also have a high degree of identity. The baboon predicted GIP (1–42) amino acid sequence together with GIP and GIPR interspecies comparisons are shown in detail in Table 1.

GIP peptide continuous ICV infusion experiments. Preliminary studies were undertaken to determine an appropriate dose of ICV GIP. A dose of 20 pmol·kg^{-1}·h^{-1} was chosen for comparison with the control condition. Animals were fasted overnight. ICV infusions were undertaken on two occasions in each animal at 0 (aCSF control) and 20 pmol·kg^{-1}·h^{-1} beginning at 2.0 h before the initiation of the mixed meal tolerance tests. On each occasion, a baseline (fasted, pre-ICV infusion) venous blood sample was taken at −135 min from the initiation of the meal test (0 min) and a syringe containing the given GIP dose was loaded on the syringe pump. At −120 min, the ICV infusion was initiated remotely at a continuous infusion rate of 10 μl/h for each dose beginning with a 30-min priming infusion to clear the ICV line dead space. Hence, ICV infusions were timed according to measured dead space volume of each infusion line such that GIP entered the ventricles 90 min before the start of the meal test. Each infusion condition was conducted 1 wk apart, and the dose order was randomized. All animals were tested in the fully conscious and alert state.

Mixed meal test. Solid mixed meals were made using peanut butter, graham crackers, and regular butter mixed to form small solid spheres of ~5 cm in diameter. Each mixed meal was presented to the baboon in the form of three balls. Each complete meal contained 45% fat,

Table 1. *GIP and GIPR phylogenetic analysis summary*

	GIP (1–42) Amino Acid Sequences
GIP-Hs	YAEGTFISDYSIAMDKIHQQDFVNWLLAQKGKKNDWKHNITQ
GIP-Ph	YAEGTFISDYSIAMDKIHQQDFVNWLLAQKGKKNDWKHNITQ
GIP-cf.	YAEGTFISDYSIAMDKI**R**QQDFVNWLLAQKGKKNDWKHNITQ
GIP-Rn	YAEGTFISDYSIAMDKI**R**QQDFVNWLLAQKGKKNDWKHN**L**TQ

	Predicted GIP (1–42) Amino Acid Sequence Identity Among Species, %			
	GIP-Rn	GIP-cf.	GIP-Hs	GIP-Ph
GIP-Rn	100.0			
GIP-cf.	97.6	100.0		
GIP-Hs	95.2	97.6	100.0	
GIP-Ph	95.2	97.6	100.0	100.0

	Predicted GIPR (1–466) Amino Scid Sequence Identity Among Species, %			
	GIPR-Rn	GIPR-cf.	GIPR-Hs	GIPR-Ph
GIPR-Rn	100.0			
GIPR-cf.	80.8	100.0		
GIPR-Hs	81.3	86.6	100.0	
GIPR-Ph	81.1	86.1	96.8	100.0

GIP, glucose-dependent insulinotropic polypeptide; GIPR, GIP receptor; Rn, *Rattus norvegicus* (rat); cf., *Canis lupus familiaris* (dog); Hs, *Homo sapiens* (human); Ph, *Papio hamadryas* (baboon). The underlined amino acids denote differences from the human sequence.

45% carbohydrate, and 10% protein as total energy and were designed to provide each baboon with 15 kcal and 1.5 g glucose per kilogram of body weight. As described above, all animals were exposed to the mixed meal before the initiation of the ICV experiments.

After an overnight fast of 14 h, baseline fasted venous blood samples were taken at −30 and −15 min before the administration of the mixed meal test. The meal was presented to the baboon in three pieces over a 5-min period. Consumption of each piece of the meal was observed and confirmed remotely using a networked video camera animal monitoring system. Serial venous blood samples were taken at 10, 20, 30, 45, 60, 90, 120, 180, and 300 min. after the meal presentation. The ICV infusion was continued until completion of the meal test at 300 min.

Peptide and metabolic substrate assays. Plasma concentrations of glucose and triglyceride were determined using an ACE clinical chemistry analyzer (Alfa Wasserman Diagnostic Technologies, West Caldwell, NJ). Plasma nonesterified free fatty acids were measured using colorimetric kits (NEFA-HR, Wako Diagnostics, Mountain View, CA). Plasma insulin was determined using a DPC Immulite 1000 Analyzer (Diagnostics Products, Los Angeles, CA). Plasma glucagon was measured using a commercial radioimmunoassay (GL-32K, EMD Millipore Diagnostics, Billerica, MA). Plasma total GIP and total pancreatic polypeptide (PP) were measured in plasma using commercial ELISA kits (EZHGIP-54K and EZHPP-40K, EMD Millipore Diagnostics). All ELISA kits used were for the detection of human forms of the peptides. Laboratory intra- and interassay coefficients of variation were <15% for all immunoassays undertaken.

Gene sequencing. Total RNA was isolated from frozen tissue (gastrointestinal and pancreas) using TRIzol Reagent (ThermoFisher Scientific, Walthman, MA). RNA was treated with RQ1 DNAse (Promega, Madison, WI) for 15 min at 37°C to remove traces of genomic DNA. For the assessment of RNA purity and integrity, we used standard methods of spectrophotometry and gel electrophoresis, respectively. cDNA was synthesized using total RNA (0.5 μg), a High Capacity cDNA Reverse Transcription kit (ThermoFisher Scientific), and oligo(dT) 12-18 primer (ThermoFisher Scientific) in 30 μl of total reaction volume. A primer set to amplify baboon GIP and GIPR transcripts was designed using human and macaque sequences as templates. For GIP, the sense primer was 5′-TCTGGAAGAGCTGGAAAGGA-3′ and the antisense primer was 5′-CTATTCTGGAGTGGGGCTGA-3′; for GIPR, the sense primer was 5′-ATTGAGTGCCTACTGCGTGC-3′ and the antisense primer was 5′-TACACGAACCAGACCCTTCG-3′. PCR was carried out using 100 ng cDNA, 0.4 μM of each primer, and the GoTaq PCR master mix kit (Promega). The amplification reaction was carried out in a thermal cycler (Veriti 96-well Thermal Cycler, ThermoFisher Scientific). The amplification program used was as follows: an initial denaturation step of 4 min at 94°C, 35 cycles of 30 s each at 94°C, 45 s at 60°C, and 90 s at 72°C, and finally an elongation step of 6 min at 72°C. PCR products were visualized on 1.0% agarose gels stained with ethidium bromide and visualized under ultraviolet light. The amplified products were cloned in the 3.5-kb XL-TOPO vector and transformed into the electrocompetent *Escherichia coli* bacteria strain, One Shot TOP10, according to the manufacturer's specifications (Invitrogen, Carlsbad, CA). Positive clones were sequenced using Big Dye Terminator Cycle Sequencing Kit version 3.1 using specific oligos and/or M13 universal primers. Reactions were analyzed in the ABI PRISM 3100 Genetic Analyzer using Sequencing Analysis Software version 5.3 (Applied Biosystems, Foster City, CA). The information obtained from the sequencing assays was subjected to a BLAST test to determine identity.

Quantitative real-time PCR. Hypothalamus and pancreatic tissues were collected in liquid N_2 during routine necropsies (colony management) in three baboons (not those used in the ICV infusion experiments). Total RNA was extracted from the hypothalamus and pancreas samples using TRIzol Reagent (Molecular Research Center, Gaithersburg, MD) and treated with RQ1 DNAse to remove contaminating genomic DNA. The quality of the RNA was determined via ultraviolet light at 230, 260, and 280 nm, and its integrity was ascertained by staining with ethidium bromide on a 1.2% agarose gel. Quantitative real-time PCR was carried out in the Applied Biosystems 7000 real-time PCR System. TaqMan Gene Expression Assays (Applied Biosystems) were specifically designed to amplify GIPR and glucagon-like peptide-1 receptor (GLP1R) transcripts. GIPR and GLP1R amplifications were performed using available commercial primers and a probe (Assay ID Hs006092_m1 and Hs00157705_m1, Applied Biosystems). 18S rRNA was chosen as the internal control. Multiplex reactions consisted of 12.5 μl of 2× TaqMan Universal PCR master mix, 1.25 μl of each 20× assay on demand, 1.5 μl of cDNA, and water to complete 25-μl final volume. PCR parameters were 50°C for 2 min and 95°C for 10 min followed by 50 cycles at 95°C for 15 s and 60°C for 1 min. Validation experiments were performed to verify that the amplification efficiency of the control was similar to that of the target genes. A cycle threshold (C_T) value in the linear range of amplification was selected for each sample in triplicate and normalized to 18S expression levels (ΔC_T).

Phylogenetic analysis. Sequences obtained from clones were aligned with the orthologous reported genes in GenBank: GIP (*Rattus norvegicus*: XM_008767947, *Canis lupus familiaris*: XM_003639272, and *Homo sapiens*: NM_004123) and GIPR (*Rattus norvegicus*: NM_012714, *Canis lupus familiaris*: XM_014119625, and *Homo sapiens*: NM_000164) using the CLUSTAL W program. Peptide and protein sequences were derived by conceptual translation of the coding sequences.

Statistical analysis. The area under the curve (AUC) was calculated using the trapezoidal method with linear interpolation between points. The following AUC variables were analyzed: *1*) total AUC (total area under the curve representing the complete integral of GIP concentrations measured over the entire experimental period of 435 mins), *2*) postprandial AUC (the area under the curve of the postprandial period from before meal administration to 300min), and *3*) postprandial iAUC(the incremental area under the curve above fasted, baseline values). All variables were transformed using Box-Cox transformations to meet assumptions of Gaussian normality before statistical analysis. Control condition and test condition means were compared

Table 2. *Baseline characteristics and fasted metabolic profiles*

	Means ± SD	Minimum-Maximum
Body weight, kg	28.9 ± 2.1	26.5–30.6
Glucose, mg/dl	92.3 ± 1.3	91.0–94.0
GIP, pg/ml	64.4 ± 6.4	55.7–70.9
Insulin, μU/ml	20.2 ± 2.2	17.1–22.3
C-peptide, ng/ml	0.490 ± 0.266	0.250–0.667
GLN, pg/ml	120.3 ± 14.1	100.4–130.7
PP, pg/ml	51.9 ± 25.7	15.8–73.4
TG, mg/dl	34.4 ± 3.6	29.3–37.3
NEFA, meq/l	0.260 ± 0.085	0.168–0.372

$n = 3$. GLN, glucagon; PP, pancreatic polypeptide; TG, triglyceride; NEFA, nonesterified free fatty acids.

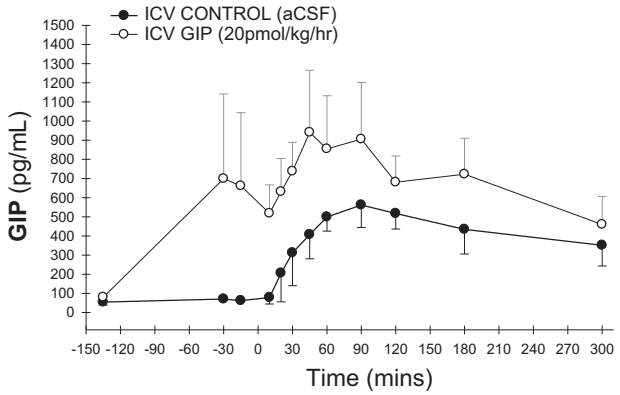

Fig. 2. Effect of intracerebroventricular (ICV) glucose-dependent insulinotropic polypeptide (GIP) on plasma GIP. Plasma GIP concentrations under continuous ICV artificial cerebrospinal fluid (aCSF) infusion and under continuous ICV GIP infusion over the experimental period are shown. ICV GIP infusion was initiated at time = −120 min, and the meal test was administered at time = 0 min. Data are means ± SE; $n = 3$.

using paired *t*-tests. Analyses were undertaken using XLSTAT version 2015.5.01.23261 (Addinsoft). A two-tailed α level of 0.05 was used to determine the statistical significance in all tests.

RESULTS

Basic descriptive data are shown in Table 2. The baboons were young adult male baboons (7–11 yr old) with normal body weight and normal metabolic status. Body weight was stable during the testing period (Fig. 1, *bottom*). No behavioral abnormalities were noted during any of the experiments; although normal food was withheld during the experimental periods, food intake after all of the experimental periods was normal. Normal hematology and biochemistry values were present throughout the study period. One animal did not go forward into the experimental phase of the study because of system compatibility issues and was released from study. Data on this animal are not included, and data from the remaining $n = 3$ animals were analyzed.

Fasted GIP concentrations and GIP AUC values are shown in Table 3. ICV GIP infusion resulted in significantly higher mean fasted GIP concentrations ($P = 0.04$). Mean ± SE GIP concentrations under control and ICV GIP conditions are shown in Fig. 2. The significantly higher total AUC GIP indicated that GIP remained elevated for the duration of the experimental period ($P < 0.05$). The GIP AUC for the postprandial period was also higher under ICV GIP and but did not reach statistical significance ($P = 0.057$). The GIP iAUC for the postprandial period was not different under ICV GIP ($P = 0.45$; Table 3), indicating that the effect on fasted GIP accounted for the entire increased GIP response over the duration of the experimental period.

Fasted insulin and insulin AUCs are shown in Table 4. Fasted insulin did not differ between control and ICV GIP conditions. Total insulin AUC and postprandial insulin AUC were not significantly different between control and stimulated conditions. However, the postprandial insulin iAUC was significantly higher (48%) under the ICV GIP infusion ($P = 0.01$; Table 4). Mean ± SE INS concentrations over the experimental period in control and ICV GIP condition are shown in Fig. 3*A*.

Fasted glucagon and glucagon AUCs are shown in Table 4. Fasted glucagon concentrations were unaffected by ICV GIP administration. Postprandial glucagon concentrations did not differ between control and ICV GIP conditions. Glucagon total AUC was also unaffected by the ICV GIP infusion. Mean ± SE glucagon concentrations over the experimental period are shown in Fig. 3*B*.

Fasted PP and PP AUCs are shown in Table 4. Fasted PP was higher under ICV GIP, but the difference did not reach statistical significance ($P = 0.23$). With ICV GIP infusion, PP concentrations were significantly higher (30.1% and 32.7%) across both the entire experimental period ($P = 0.003$) and postprandial period ($P = 0.037$), although the incremental postprandial PP increase did not reach statistical significance (60.4%, $P = 0.18$). Mean ± SE PP concentrations over the experimental period are shown in Fig. 3*C*.

Glucose, triglyceride, and free fatty acid concentrations in the fasted AUCs are shown in Table 5. Neither fasted glucose, triglyceride, nor free fatty acid concentrations differed under conditions of ICV GIP and ICV aCSF. Similarly, there were no significant differences in the three variables across the experimental period or in the postprandial period.

Table 3. *Effects of intracerebroventricular GIP administration on fasted GIP, total GIP, and postprandial GIP concentrations*

	Control (aCSF)	GIP (20 pmol·kg^{-1}·h^{-1})	*P* Value
Fasted GIP, pg/ml	66.5 ± 8.0	680.6 ± 412.8	0.047*
Total GIP AUC, pg·ml^{-1}·min	724 ± 136	3,437 ± 2514	0.041*
Postprandial GIP AUC, pg·ml^{-1}·min	417.6 ± 133.7	728.5 ± 261.5	0.057
Postprandial GIP iAUC, pg·ml^{-1}·min	351.2 ± 139.2	255.2 ± 224.5	0.448

Data are means ±SD. Fasted values were calculated as the average peptide concentration at the −30- and −15-min time points. Total area under the curve (AUC) was calculated as the total AUC from −135 to 300 min. aCSF, artificial cerebrospinal fluid; iAUC, incremental area under the curve. *P* values are for means comparisons using paired *t*-tests. *Statistically significant.

Table 4. *Effects of intracerebroventricular GIP administration on pancreatic islet peptide secretion*

	Control (aCSF)	GIP (20 pmol·kg^{-1}·h^{-1})	*P* Value
Fasted insulin, μU/ml	12.8 ± 5.5	15.9 ± 7.3	0.330
Total insulin AUC, μU·ml^{-1}·min	19,880 ± 4,524	26,361 ± 9,440	0.123
Postprandial insulin AUC, μU·ml^{-1}·min	11,910 ± 3,210	16,140 ± 5,510	0.152
Postprandial insulin iAUC, μU·ml^{-1}·min	8,130 ± 3,690	12,030 ± 3,708	0.010*
Fasted GLN, pg/ml	109.9 ± 10.3	99.1 ± 13.0	0.450
Total GLN AUC, pg·ml^{-1}·min	38,889 ± 6,917	46,719 ± 10,875	0.599
Postprandial GLN AUC, pg·ml^{-1}·min	25,920 ± 4,200	33,420 ± 9,150	0.741
Fasted PP, pg/ml	35.7 ± 28.2	59.6 ± 11.7	0.229
Total PP AUC, pg·ml^{-1}·min	42,369 ± 16,965	55,115 ± 20,184	0.003*
Postprandial PP AUC, pg·ml^{-1}·min	37,560 ± 15,480	49,830 ± 19,530	0.037*
Postprandial PP iAUC, pg·ml^{-1}·min	23,790 ± 14,160	38,160 ± 20,550	0.181

Data are means ± SD. Fasted values were calculated as the average peptide concentration at the −30- and −15-min time points. Total AUC was calculated as the total AUC from −135 to 300 min. iAUC was not reported for GLN as values were below baseline during the postprandial period. *P* values are for means comparisons using paired *t*-tests. *Statistically significant.

In a separate experiment, GIPR and GLP1R gene expression were quantified in hypothalamus tissues and compared with pancreas tissues collected from three baboons (2 female baboons and 1 male baboon). Transcript expression quantifications are shown in Fig. 4. The GIPR transcript was expressed in the baboon hypothalamus and was present in quantities similar to that of GLP1R.

DISCUSSION

GIP exerts complex pleiotropic actions on whole body metabolism. The abundant and extensive distribution of GIP and its receptor in the brain suggests important functions of central nervous system GIP signaling. Our data demonstrate that central GIP signaling can promote increased plasma GIP concentrations independent of nutrient stimulation and increase insulin and PP responses to a meal challenge. These data provide the first evidence for peripheral metabolic actions generated by GIP signaling in the central nervous system.

Multiple studies have provided evidence that GIP functions as a signaling molecule in the central nervous system. The GIPR transcript and protein are found in multiple regions of the rat central nervous system and have also been identified in the hippocampus and temporal lobe of humans (23). Importantly, neural cells expressing GIP have also been identified in the rat brain, particularly in the olfactory bulb, hippocampus, hypothalamus, thalamus, and cerebellum (36). The available data are consistent with central GIP having neurotrophic effects together with effects on synaptic plasticity and central nervous system inflammation. ICV administration of GIP (1.92 nmol/day) for 5 days increased the proliferation of hippocampal progenitor cells (37), whereas acute ICV GIP administration (15 nmol) preserved long-term potentiation, suggesting an improvement in synaptic plasticity in response to GIP in rats (24). Chronic peripheral administration of a long-lasting GIP analog prevented the decrease in long-term potentiation induced by high-fat feeding in rats and improved object recognition memory and reduced oxidative stress and inflammation in both the cortex and hippocampus of mice (18, 34). Consistent with the aforementioned findings, GIPR knockout mice show a reduction in recognition and spatial learning and exhibit a reduced long-term potentiation in the hippocampus (20). Therefore, effects of GIP on central nervous system function have been well described.

Here, we provide evidence for a brain-gut axis signal generated by central GIP signaling that promotes an increase in peripheral GIP concentrations in the absence of nutrient stimulation. Presumably, the signal is transmitted through an efferent neural pathway capable of interacting with intestinal K cells. Consistent with our findings, brain insulin signaling has been shown to generate a signal that promotes its own secretion from the β-cell (10, 47, 49). As with insulin action in the brain, the physiological significance of central GIP action is also unclear, and it is not known whether circulating GIP can cross the blood-brain barrier. Nevertheless, GIP analogs exerted central nervous system effects when administered peripherally to rodents, suggesting that GIP can cross the blood-brain barrier (39). Studies undertaken in dogs have provided strong evidence for a brain-gut signaling pathway capable of modulating GIP concentrations in the peripheral circulation. Plasma GIP concentrations were increased by ICV administration of neuropeptide Y (25-μg bolus) independent of any nutrient stimulation (48). Furthermore, ICV neurotensin (1,000 ng·kg^{-1}·h^{-1}) and bombesin (5.4 ng·kg^{-1}·h^{-1}) also increased plasma GIP concentrations in both the fasted condition and under duodenal glucose stimulation (50, 51): the GIP increase in these studies was less than that observed under ICV neuropeptide Y. Overall, the ICV effects of these peptides on fasted GIP were 50–70% less than those seen in our study. Interestingly, ICV insulin reduced GIP concentrations but only during nutrient stimulation (49). The nature of the putative efferent pathway that mediates this effect remains unknown.

Our data add to the current literature on the metabolic effects of central GIP signaling. One prior study has described an effect of ICV GIP on energy balance (2). Four days of ICV GIP infusion (2 nmol/day) in rats resulted in changes in the expression of genes associated with metabolic regulation in the hypothalamus, including neuropeptide Y, and led to weight loss without changes in food intake, but circulating metabolic peptides were not measured (2). Our acute infusion experiments were not designed to address effects of ICV GIP on body weight regulation, but such studies are warranted in higher species. In support,

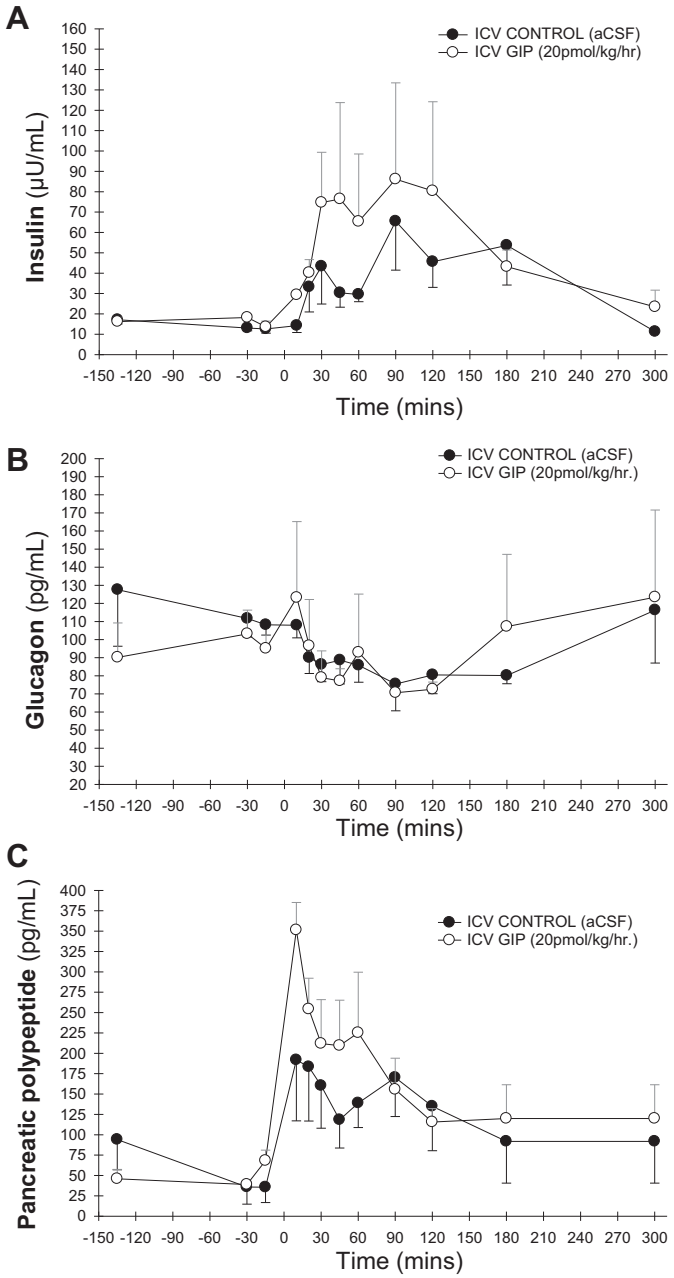

Fig. 3. Effect of ICV GIP on plasma insulin, glucagon, and pancreatic polypeptide. *A*: plasma insulin concentrations under continuous ICV aCSF infusion and under continuous ICV GIP infusion over the experimental period. ICV GIP infusion was initiated at time = −120 min, and the meal test was administered at time = 0 min. Data are means ± SE; $n = 3$. *B*: plasma glucagon concentrations under continuous ICV aCSF infusion and under continuous ICV GIP infusion over the experimental period. ICV GIP infusion was initiated at time = −120 min, and the meal test was administered at time = 0 min. Data are means ± SE; $n = 3$. *C*: plasma pancreatic polypeptide concentrations under continuous ICV aCSF infusion and under continuous ICV GIP infusion over the experimental period. ICV GIP infusion was initiated at time = −120 min, and the meal test was administered at time = 0 min. Data are means ± SE; $n = 3$.

our quantitative real-time PCR assays were positive for GIPR gene expression in baboon hypothalamic tissue (Fig. 4). We found that hypothalamic expression of GIPR in the baboon was comparable with that of GLP1R, which is known to have hypothalamic expression and function.

Our data are consistent with the presence of an efferent neural signaling system directly regulating GIP release from intestinal enteroendocrine cells. Consistent with the increase in plasma GIP, the principal finding of the study, we also found evidence for increased postprandial plasma insulin and PP concentrations with ICV GIP infusion. An increase in PP is typically taken to reflect an increase in cholinergic input to the pancreatic islets (42). Conflicting data have been published regarding the influence of the parasympathetic nervous system on GIP release (52), but the weight of evidence favors noncholinergic involvement in GIP secretion. Moreover, evidence from human studies indicates that peripheral GIP administration increases PP concentrations (1, 11, 13). Therefore, the most parsimonious explanation is that the increase in PP was attributable to the increased peripheral GIP concentrations and not directly by central GIP action. Furthermore, the increase in plasma GIP was also likely to be the direct cause of the higher postprandial insulin concentrations that occurred under ICV GIP. We did not find differences in fasted or postprandial glucose concentrations in response to ICV GIP administration, but, as has been previously shown (19), only small increments in plasma glucose occur in response to oral meal challenges in healthy glucose-tolerant baboons and leave a very small window for detecting glucose-lowering effects. The evidence we show for elevations of both PP and insulin with ICV GIP suggests that central GIP signaling was able to influence both peptides indirectly by promoting peripheral GIP release.

A weakness of our study is that we were unable to quantify whether there was any GIP spillover from the CSF during our ICV infusion. Our ICV dose of GIP (100 $ng \cdot kg^{-1} \cdot h^{-1}$ or 20 $pmol \cdot kg^{-1} \cdot h^{-1}$) was chosen based on assessments of ICV peptide administration to nonhuman primates, dogs, and rodents. The chosen dose was approximately one order of magnitude less than the typical ICV dose administered in the aforementioned rodent studies (2, 37). For example, the dose of ICV GIP administered to rats by Nyberg et al. was 14 times greater than the dose we used in baboons after accounting for body weight and, hence, ventricular and CSF volume differences (37). In humans, a direct intravenous infusion of GIP at a dose three times that chosen in our study was required to raise plasma total GIP concentrations up to a maximum of ≈50% of those seen in our study (30). Furthermore, in a study by Chia et al. (12) in humans, a 12-fold higher intravenous GIP infusion rate than the ICV infusion rate we used in baboons resulted in a 10-fold increase in plasma total GIP from baseline, which is comparable to the plasma GIP increase that we observed in baboons. Therefore, it is unlikely that our dose of GIP was large enough and unlikely that it would have entered the vasculature fast enough to explain the rate and extent of the plasma GIP increase observed. Furthermore, a 2.0 $pmol \cdot kg^{-1} \cdot h^{-1}$ ICV dose of GIP, used during preliminary experiments, resulted in a GIP increase of ≈30% of that caused by the 20 $pmol \cdot kg^{-1} \cdot h^{-1}$ dose and is consistent with a dose response to ICV GIP (data not shown).

Nonhuman primates are important intermediary models for the translation of rodent findings to humans. Given the particular importance of nonhuman primates as translational models for metabolic diseases (7, 40), investigations to

Table 5. *Effects of intracerebroventricular GIP administration on plasma glucose, triglyceride, and free fatty acid concentrations*

	Control (aCSF)	GIP (20 pmol·kg^{-1}·h^{-1})	*P* Value
Fasted glucose, mg/dl	91.7 ± 3.3	93.0 ± 2.9	0.643
Total glucose AUC, mg·dl^{-1}·min	307,452 ± 8,557	300,597 ± 2,711	0.403
Postprandial glucose AUC, mg·dl^{-1}·min	29,164 ± 2,241	30,049 ± 540	0.503
Postprandial glucose iAUC, mg·dl^{-1}·min	1,664 ± 1,483	2,149 ± 798	0.370
Fasted TG, mg/ml	33.7 ± 7.2	32.5 ± 3.5	0.743
Total TG AUC, mg·dl^{-1}·min	116,627 ± 19,047	109,836 ± 9,177	0.614
Postprandial TG AUC, mg·dl^{-1}·min	11,610 ± 2,834	10,981 ± 1,342	0.769
Postprandial TG iAUC, mg·dl^{-1}·min	1,819 ± 1,652	1,552 ± 1,414	0.752
Fasted NEFA, meq/l	0.244 ± 0.061	0.284 ± 0.061	0.517
Total NEFA AUC, meq·l^{-1}·min	827.0 ± 248.2	885.3 ± 181.4	0.751
Postprandial NEFA AUC, meq·l^{-1}·min	58.8 ± 3.6	62.6 ± 15.5	0.738

Data are means ± SD. Fasted values were calculated as the average concentration at the −30- and −15-min time points. Total AUC was calculated as the total AUC from −135 to 300 min. iAUC was not reported for NEFA as values were below baseline during the postprandial period. *P* values are for means comparisons using paired *t*-tests.

confirm that gut-brain and brain-gut signaling pathways found in rodents are operative in nonhuman primates is of considerable importance. The baboon model is well established in the study of all stages of metabolic disease (9, 19, 25, 26, 28, 46). Our ICV infusion methodology advances previously described ICV infusion techniques applied in conscious nonhuman primates (3, 4, 43). The externalization of the ICV cannula line to a remotely controlled pump enables more control over the ICV infusion and readily permits acute or continuous chronic studies with minimal disturbance to the animal. Prior studies of this nature typically enabled only bolus ICV administrations (33) or chronic infusions to be undertaken using implantable osmotic pumps (3, 4, 43). The ICV infusion system described here enables greater control over the dose quantity, timing, and duration.

In summary, we found that ICV administered GIP increased peripheral GIP concentrations and influenced postprandial islet peptide secretion in nonhuman primates. Our data are the first to demonstrate a role for central GIP action in the regulation of peripheral GIP release and the first to show that central GIP action can influence islet peptide secretion.

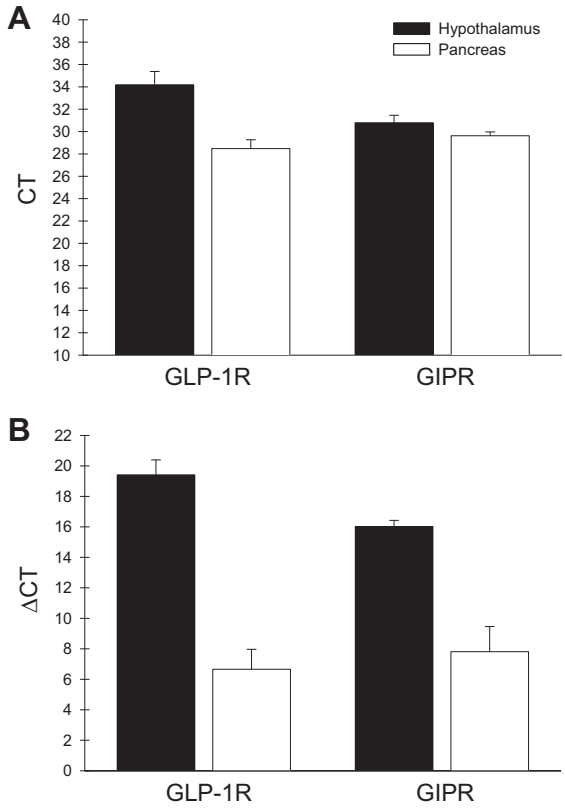

Fig. 4. Glucose-dependent insulinotropic polypeptide receptor (GIPR) gene expression relative to glucagon-like peptide 1 receptor (GLP-1R) expression in the hypothalamus and pancreas of baboons ($n = 3$) by quantitative real-time PCR. *A*: mean ± SE cycle threshold (C_T) values. *B*: mean ± SE ΔC_T values (normalized to 18S expression).

ACKNOWLEDGMENTS

The authors gratefully acknowledge the expert technical assistance of David Weaver in implementing the tether system modifications and in the habituation, management, and care of the study animals. The authors thank Vicki Mattern for conducting all laboratory assays. The authors also thank the Southwest National primate Research Center veterinarians Dr. Patrice Frost and Dr. Cassondra Bauer for the surgical expertise and care and management of the animals throughout the study. The authors acknowledge the contributions of Dr. Andrea Mari to the critical appraisal of the data and revisions to the manuscript.

GRANTS

Direct costs of the study were supported by a grant from the Kronkosky Foundation (San Antonio, TX) Health and Human Services Program. This investigation used resources that were supported by Southwest National Primate Research Center Grant P51-OD-011133 from the Office of Research Infrastructure Programs (ORIP) of the National Institutes of Health (NIH). This investigation was conducted in facilities constructed with support from ORIP of NIH through Grants C06-RR-014578, C06-RR-013556, C06-RR-015456, and C06-RR-017515.

DISCLOSURES

No conflicts of interest, financial or otherwise, are declared by the author(s).

AUTHOR CONTRIBUTIONS

P.B.H. and R.E.S. conception and design of research; P.B.H., R.E.S., I.P.R.-S., M.G.-F., V.S.V., and S.A.C. performed experiments; P.B.H. analyzed data; P.B.H., R.E.S., I.P.R.-S., M.E.T.-B., A.G.C., and F.F. interpreted results of experiments; P.B.H. prepared figures; P.B.H. and F.F. drafted manuscript; P.B.H., R.E.S., A.G.C., and F.F. edited and revised manuscript; P.B.H., R.E.S., I.P.R.-S., M.G.-F., M.E.T.-B., V.S.V., S.A.C., A.G.C., and F.F. approved final version of manuscript.

REFERENCES

1. **Ahrén B, Pettersson M, Uvnäs-Moberg K, Gutniak M, Efendic S.** Effects of cholecystokinin (CCK)-8, CCK-33, and gastric inhibitory polypeptide (GIP) on basal and meal-stimulated pancreatic hormone secretion in man. *Diabetes Res Clin Pract* 13: 153–161, 1991.
2. **Ambati S, Duan J, Hartzell DL, Choi YH, Della-Fera MA, Baile CA.** GIP-dependent expression of hypothalamic genes. *Physiol Res* 60: 941–50, 2011.
3. **Blair-West JR, Carey KD, Denton DA, Weisinger RS, Shade RE.** Evidence that brain angiotensin II is involved in both thirst and sodium appetite in baboons. *Am J Physiol Regul Integr Comp Physiol* 275: R1639–R1646, 1998.
4. **Blair-West JR, Carey KD, Denton DA, Madden LJ, Weisinger RS, Shade RE.** Possible contribution of brain angiotensin III to ingestive behaviors in baboons. *Am J Physiol Regul Integr Comp Physiol* 281: R1633–R1636, 2001.
5. **Brown JC, Pederson RA, Jorpes E, Mutt V.** Preparation of highly active enterogastrone. *Can J Physiol Pharmacol* 47: 113–114, 1969.
6. **Burcelin R.** The gut-brain axis: a major glucoregulatory player. *Diabetes Metab* 36, *Suppl* 3: S54–S58, 2010.
7. **Cabrera O, Berman DM, Kenyon NS, Ricordi C, Berggren PO, Caicedo A.** The unique cytoarchitecture of human pancreatic islets has implications for islet cell function. *Proc Natl Acad Sci USA* 103: 2334–2339, 2006.
8. **Campbell JE, Drucker DJ.** Pharmacology, physiology, and mechanisms of incretin hormone action. *Cell Metab* 17: 819–37, 2013.
9. **Chavez AO, Lopez-Alvarenga JC, Tejero ME, Triplitt C, Bastarrachea RA, Sriwijitkamol A, Tantiwong P, Voruganti VS, Musi N, Comuzzie AG, DeFronzo RA, Folli F.** Physiological and molecular determinants of insulin action in the baboon. *Diabetes* 57: 899–908, 2008.
10. **Chen M, Woods SC, Porte D Jr.** Effect of cerebral intraventricular insulin on pancreatic insulin secretion in the dog. *Diabetes* 24: 910–914, 1975.
11. **Chia CW, Odetunde JO, Kim W, Carlson OD, Ferrucci L, Egan JM.** GIP contributes to islet trihormonal abnormalities in type 2 diabetes. *J Clin Endocrinol Metab* 99: 2477–2485, 2014.
12. **Chia CW, Carlson OD, Kim W, Shin YK, Charles CP, Kim HS, Melvin DL, Egan JM.** Exogenous glucose-dependent insulinotropic polypeptide worsens post prandial hyperglycemia in type 2 diabetes. *Diabetes* 58: 1342–1349, 2009.
13. **Chowdhury S, Wang S, Patterson BW, Reeds DN, Wice BM.** The combination of GIP plus xenin-25 indirectly increases pancreatic polypeptide release in humans with and without type 2 diabetes mellitus. *Regul Pept* 187: 42–50, 2013.
14. **Coelho AM Jr, Carey KD.** A social tethering system for nonhuman primates used in laboratory research. *Lab Anim Sci* 40: 388–394, 1990.
15. **Davis R, Huffman RD.** *A Stereotaxic Atlas of the Brain of the Baboon* (**Papio**). Austin, TX: Univ. of Texas Press, 1968.
16. **Ding KH, Zhong Q, Xie D, Chen HX, Della-Fera MA, Bollag RJ, Bollag WB, Gujral R, Kang B, Sridhar S, Baile C, Curl W, Isales CM.** Effects of glucose-dependent insulinotropic peptide on behavior. *Peptides* 27: 2750–2755, 2006.
17. **Drucker DJ.** Incretin action in the pancreas: potential promise, possible perils, and pathological pitfalls. *Diabetes* 62: 3316–23, 2013.
18. **Duffy AM, Hölscher C.** The incretin analogue D-Ala2GIP reduces plaque load, astrogliosis and oxidative stress in an APP/PS1 mouse model of Alzheimer's disease. *Neuroscience* 228: 294–300, 2013.
19. **Fabbrini E, Higgins PB, Magkos F, Bastarrachea RA, Voruganti VS, Comuzzie AG, Shade RE, Gastaldelli A, Horton JD, Omodei D, Patterson BW, Klein S.** Metabolic response to high-carbohydrate and low-carbohydrate meals in a nonhuman primate model. *Am J Physiol Endocrinol Metab* 304: E444–E451, 2013.
20. **Faivre E, Gault VA, Thorens B, Hölscher C.** Glucose-dependent insulinotropic polypeptide receptor knockout mice are impaired in learning, synaptic plasticity, and neurogenesis. *J Neurophysiol* 105: 1574–1580, 2011.
21. **Faivre E, Hamilton A, Hölscher C.** Effects of acute and chronic administration of GIP analogues on cognition, synaptic plasticity and neurogenesis in mice. *Eur J Pharmacol* 674: 294–306, 2012.
22. **Figueiredo CP, Pamplona FA, Mazzuco TL, Aguiar AS Jr, Walz R, Prediger RD.** Role of the glucose-dependent insulinotropic polypeptide and its receptor in the central nervous system: therapeutic potential in neurological diseases. *Behav Pharmacol* 21: 394–408, 2010.
23. **Figueiredo CP, Antunes VL, Moreira EL, de Mello N, Medeiros R, Di Giunta G, Lobão-Soares B, Linhares M, Lin K, Mazzuco TL, Prediger RD, Walz R.** Glucose-dependent insulinotropic peptide receptor expression in the hippocampus and neocortex of mesial temporal lobe epilepsy patients and rats undergoing pilocarpine induced status epilepticus. *Peptides* 32: 781–789, 2011.
24. **Gault VA, Hölscher C.** Protease-resistant glucose-dependent insulinotropic polypeptide agonists facilitate hippocampal LTP and reverse the impairment of LTP induced by β-amyloid. *J Neurophysiol* 99: 1590–1595, 2008.
25. **Guardado-Mendoza R, Davalli AM, Chavez AO, Hubbard GB, Dick EJ, Majluf-Cruz A, Tene-Perez CE, Goldschmidt L, Hart J, Perego C, Comuzzie AG, Tejero ME, Finzi G, Placidi C, La Rosa S, Capella C, Halff G, Gastaldelli A, DeFronzo RA, Folli F.** Pancreatic islet amyloidosis, beta-cell apoptosis, and alpha-cell proliferation are determinants of islet remodeling in type-2 diabetic baboons. *Proc Natl Acad Sci USA* 106: 13992–13997, 2009.
26. **Higgins PB, Rodriguez PJ, Voruganti VS, Mattern V, Bastarrachea RA, Rice K, Raabe T, Comuzzie AG.** Body composition and cardiometabolic disease risk factors in captive baboons (*Papio hamadryas* sp.): sexual dimorphism. *Am J Phys Anthropol* 153: 9–14, 2014.
27. **Higgins PB, Bauer C, Folli F, Garcia-Forey M, Voruganti VS, Bastarrachea RA, Nathanielsz PW, Shade RE, Comuzzie AG.** Methodology for performing intracerebroventricular infusions during metabolic studies in conscious non-human primates (Abstract). *Obesity* 19: S93–S94, 2011.
28. **Higgins PB, Bastarrachea RA, Lopez-Alvarenga JC, Garcia-Forey M, Proffitt JM, Voruganti VS, Tejero ME, Mattern V, Haack K, Shade RE, Cole SA, Comuzzie AG.** Eight week exposure to a high sugar high fat diet results in adiposity gain and alterations in metabolic biomarkers in baboons (*Papio hamadryas* sp.). *Cardiovasc Diabetol* 9: 71, 2010.
29. **Hölscher C.** The incretin hormones glucagon-like peptide 1 and glucose-dependent insulinotropic polypeptide are neuroprotective in mouse models of Alzheimer's disease. *Alzheimers Dement* 10, *Suppl* 1: S47–S54, 2014.
30. **Idorn T, Knop FK, Jørgensen MB, Christensen M, Holst JJ, Hornum M, Feldt-Rasmussen B.** Elimination and degradation of glucagon-like peptide-1 and glucose-dependent insulinotropic polypeptide in patients with end-stage renal disease. *J Clin Endocrinol Metab* 99: 2457–2466, 2014.
31. **Ji C, Xue GF, Li G, Li D, Hölscher C.** Neuroprotective effects of glucose-dependent insulinotropic polypeptide in Alzheimer's disease. *Rev Neurosci* 27: 61–70, 2016.
32. **Kaplan AM, Vigna SR.** Gastric inhibitory polypeptide (GIP) binding sites in rat brain. *Peptides* 15: 297–302, 1994.
33. **Koegler FH, Grove KL, Schiffmacher A, Smith MS, Cameron JL.** Central melanocortin receptors mediate changes in food intake in the rhesus macaque. *Endocrinology* 142: 2586–2592, 2001.
34. **Lennox R, Moffett RC, Porter DW, Irwin N, Gault VA, Flatt PR.** Effects of glucose-dependent insulinotropic polypeptide receptor knockout and a high-fat diet on cognitive function and hippocampal gene expression in mice. *Mol Med Rep* 12: 1544–1548, 2015.
35. **Li L, Wice BM.** Bombesin and nutrients independently and additively regulate hormone release from GIP/Ins cells. *Am J Physiol Endocrinol Metab* 288: E208–E215, 2005.
36. **Nyberg J, Jacobsson C, Anderson MF, Eriksson PS.** Immunohistochemical distribution of glucose-dependent insulinotropic polypeptide in the adult rat brain. *J Neurosci Res* 85: 2099–119, 2007.
37. **Nyberg J, Anderson MF, Meister B, Alborn AM, Ström AK, Brederlau A, Illerskog AC, Nilsson O, Kieffer TJ, Hietala MA, Ricksten A, Eriksson PS.** Glucose-dependent insulinotropic polypeptide is expressed in adult hippocampus and induces progenitor cell proliferation. *J Neurosci* 25: 1816–1825, 2005.
38. **Ottlecz A, Samson WK, McCann SM.** The effects of gastric inhibitory polypeptide (GIP) on the release of anterior pituitary hormones. *Peptides* 6: 115–119, 1985.
39. **Porter DW, Irwin N, Flatt PR, Hölscher C, Gault VA.** Prolonged GIP receptor activation improves cognitive function, hippocampal synaptic plasticity and glucose homeostasis in high-fat fed mice. *Eur J Pharmacol* 65: 688–693, 2011.
40. **Pound LD, Kievit P, Grove KL.** The nonhuman primate as a model for type 2 diabetes. *Curr Opin Endocrinol Diabetes Obes* 21: 89–94, 2014.
41. **Scarlett JM, Schwartz MW.** Gut-brain mechanisms controlling glucose homeostasis. *F1000Prime Rep* 7: 12, 2015.

42. **Schwartz TW, Holst JJ, Fahrenkrug J, Jensen SL, Nielsen OV, Rehfeld JF, de Muckadell OB, Stadil F.** Vagal, cholinergic regulation of pancreatic polypeptide secretion. *J Clin Invest* 61: 781–789, 1978.
43. **Shade RE, Blair-West JR, Carey KD, Madden LJ, Weisinger RS, Denton DA.** Synergy between angiotensin and aldosterone in evoking sodium appetite in baboons. *Am J Physiol Regul Integr Comp Physiol* 283: R1070–R1078, 2002.
44. **Tian JQ, Wang Y, Lin N, Guo YJ, Sun SH, Zou DJ.** Active immunization with glucose-dependent insulinotropic polypeptide vaccine influences brain function and behaviour in rats. *Scand J Immunol* 72: 1–7, 2010.
45. **Usdin TB, Mezey E, Button DC, Brownstein MJ, Bonner TI.** Gastric inhibitory polypeptide receptor, a member of the secretin-vasoactive intestinal peptide receptor family, is widely distributed in peripheral organs and the brain. *Endocrinology* 133: 2861–2870, 1993.
46. **Vaidyanathan V, Bastarrachea RA, Higgins PB, Voruganti VS, Kamath S, DiPatrizio NV, Piomelli D, Comuzzie AG, Parks EJ.** Selective cannabinoid-1 receptor blockade benefits fatty acid and triglyceride metabolism significantly in weight-stable nonhuman primates. *Am J Physiol Endocrinol Metab* 303: E624–E634, 2012.
47. **Woods SC, Porte D Jr.** Effect of intracisternal insulin on plasma glucose and insulin in the dog. *Diabetes* 24: 905–909, 1975.
48. **Yavropoulou MP, Kotsa K, Kesisoglou I, Anastasiou O, Yovos JG.** Intracerebroventricular infusion of neuropeptide Y increases glucose dependent-insulinotropic peptide secretion in the fasting conscious dog. *Peptides* 29: 2281–2285, 2008.
49. **Yavropoulou MP, Kotsa K, Anastasiou O, O'Dorisio TM, Pappas TN, Yovos JG.** Effect of intracerebroventricular infusion of insulin on glucose-dependent insulinotropic peptide in dogs. *Neurosci Lett* 460: 148–151, 2009.
50. **Yavropoulou MP, Kotsa K, Kesisoglou I, Gotzamani-Psarakou A, Yovos JG.** Effect of intracerebroventricular infusion of neurotensin on glucose-dependent insulinotropic peptide secretion in dogs. *Peptides* 31: 150–154, 2010.
51. **Yavropoulou MP, Kotsa K, Anastasiou OE, O'Dorisio TM, Pappas TN, Yovos JG.** Intracerebroventricular infusion of bombesin modulates GIP secretion in conscious dogs. *Neuropharmacology* 58: 226–232, 2010.
52. **Yavropoulou MP, Yovos JG.** Central regulation of glucose-dependent insulinotropic polypeptide secretion. *Vitam Horm* 84: 185–201, 2010.
53. **Yu YW, Hsieh TH, Chen KY, Wu JC, Hoffer B, Greig NH, Li Y, Lai JH, Chang CF, Lin JW, Chen YH, Yang LY, Chiang YH.** Glucose-dependent insulinotropic polypeptide ameliorates mild traumatic brain injury-induced cognitive and sensorimotor deficits and neuroinflammation in rats. *J Neurotraum*; doi:10.1089/neu.2015.4229.